Growth of horizontally aligned dense carbon nanotubes from trench sidewalls

2011 Nanotechnology 22 265614

(http://iopscience.iop.org/0957-4484/22/26/265614)

Nanotechnology **22** (2011) 479502 (1pp) doi:10.1088/0957-4484/22/47/479502

Corrigendum

Growth of horizontally aligned dense carbon nanotubes from trench sidewalls
Jingyu Lu, Jianmin Miao, Ting Xu, Bin Yan, Ting Yu and Zexiang Shen 2011 *Nanotechnology* **22** 265614

Received 29 September 2011
Published 2011

The authors would like to replace the penultimate sentence of section 3 with:

Therefore, there is a defect gradient along CNTs, and accordingly, the Raman intensity ratio I_G/I_D gradually increases from their roots to tips.

The authors apologize for any inconvenience caused.

Nanotechnology **22** (2011) 265614 (6pp) doi:10.1088/0957-4484/22/26/265614

Growth of horizontally aligned dense carbon nanotubes from trench sidewalls

Jingyu Lu[1], Jianmin Miao[1], Ting Xu[1], Bin Yan[2], Ting Yu[2] and Zexiang Shen[2]

[1] School of Mechanical and Aerospace Engineering, Nanyang Technological University, Singapore
[2] School of Physical and Mathematical Sciences, Nanyang Technological University, Singapore

E-mail: mjmmiao@ntu.edu.sg

Received 8 February 2011, in final form 2 April 2011
Published 18 May 2011
Online at stacks.iop.org/Nano/22/265614

Abstract
Horizontally aligned, dense carbon nanotubes (HADCNTs) in the form of CNT cantilevers/bridges were grown from selected trench sidewalls in silicon substrate by chemical vapor deposition (CVD). The as-grown CNT cantilevers/bridges are packed with multiwalled carbon nanotubes (MWCNTs) with a linear density of about 10 CNTs μm^{-1}. The excellent horizontal alignment of these CNTs is mainly ascribed to the van der Waals interactions within the dense CNT bundles. What is more, the Raman intensity ratio I_G/I_D shows a gradual increase from the CNT roots to tips, indicating a defect gradient along CNTs generated during their growth. These results will inspire further efforts to explore the fundamentals and applications of HADCNTs.

(Some figures in this article are in colour only in the electronic version)

1. Introduction

The fantastic mechanical, electrical, thermal, and optical properties of carbon nanotubes (CNTs) have offered great potential in a wide variety of applications ranging from micro/nanodevices (for example, various sensors [1–3] and actuators [4–6]) to megastructures such as space elevators, as proposed by Pugno *et al* [7]. Recently, there has been growing interest in the development of CNT-based nanoelectronic devices, including field effect transistors [8] and horizontal interconnects [9], which require CNTs to be densely packed with good horizontal alignment.

Therefore, great efforts have been devoted to the growth of horizontally aligned, dense CNTs (HADCNTs). Depending on the dominant CNT horizontal alignment mechanism, these efforts can be categorized into four growth methods. The first approach uses gas flow to align CNTs grown with iron salt (e.g. $FeCl_3$ [10], $Fe(NO_3)_3$ [11]) or ferrocene ($Fe(C_2H_5)_2$) [12] solution as precursor, and could obtain centimeter long CNTs [10]; the second way takes advantage of the crystal lattice or atomic step on the substrate (Si [13], SiO_2 [14], Al_2O_3 [15], or MgO [16]) surface, because the van der Waals interactions between CNTs and the substrate is angle-dependent [17]; the third solution introduces a horizontal magnetic [18] or electric field [19] to guide the behavior of ferromagnetic catalysts. All these methods could obtain CNTs with a certain horizontal alignment, but most of the time, the CNT density (number of CNTs per cross-sectional width in a CNT bundle) obtained is not encouraging. To alleviate this problem, the fourth recipe was developed with the deposition of a catalyst film on substrate vertical surfaces [9, 20], because dense CNTs are prone to extrude normal to the catalyst plane [21]. However, these CNTs grew from several sidewalls at the same time. In this paper, we provide a solution to obtain HADCNTs in the form of CNT cantilevers/bridges from the selected trench sidewalls in silicon substrate, which were later characterized with scanning electron microscopy (SEM), current–voltage measurements, high resolution transmission electron microscopy (HRTEM), and Raman spectroscopy. These results will ignite further interest in the basics and applications of HADCNTs.

2. Experiment

The fabrication process is sketched in figure 1; it mainly involves the fabrication of trench structures and tilt angle

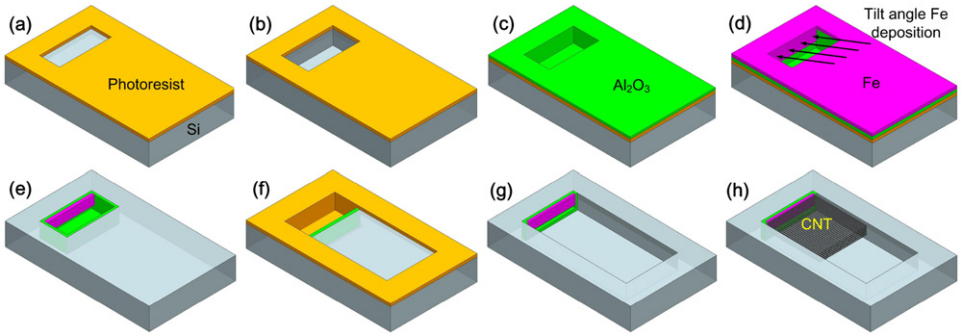

Figure 1. Schematic of the HADCNTs fabrication process: (a) photolithography patterning and (b) DRIE etching of the first trench, (c) ALD deposition of the Al_2O_3 layer and (d) tilt angle electron evaporation of the Fe catalyst layer, (e) removal of photoresist, (f) patterning of the second trench with photolithography, (g) removal of photoresist after DRIE etching of the second trench, and (h) the CVD growth of HADCNTs.

deposition of Fe catalyst onto the selected trench sidewalls. Each trench structure consists of two trenches with different widths joined together. The first trench is just about 5 μm wide, and it was created by photolithography patterning (figure 1(a)) and deep reactive ion etching (DRIE) in a silicon wafer (figure 1(b)) with a depth of about 15 μm, then a 10 nm thick Al_2O_3 layer was deposited by atomic layer deposition (ALD) to cover the trench surfaces as a buffer layer (figure 1(c)), after that, the selected sidewall (the left sidewall in figure 1) was covered with a Fe catalyst layer (nominal thickness of 2 nm) by electron beam evaporation (figure 1(d)) with a tilt angle of about 70° relative to the substrate top surface. Therefore, the first trench functions as both the hard mask and acceptor for Fe catalyst deposition. After removal of photoresist (figure 1(e)), the second trench was patterned (figure 1(f)) by photolithography and etched with much larger widths (∼5 μm–3 mm for different patterns) by the DRIE process, and there was a 2–3 μm overlap between two trenches, so that they could be connected to each other after fabrication. During the later chemical vapor deposition (CVD) process, CNTs could find a large space to grow from the left sidewall of the first trench (only ∼5 μm wide) all the way to the second trench, and thus long HADCNTs could be expected. After removal of photoresist (figure 1(g)), the wafer was diced into small pieces (∼5 mm × 10 mm) with a diamond cutter. Then some samples were put into the quartz chamber of a traditional thermal CVD system to grow CNTs.

The CNT growth took place at 750 °C and about 11 Torr gas pressure (monitored *in situ* by a Granville-Phillips Series 275 Mini-Convectron vacuum gauge). The gas mixture of $Ar/H_2/C_2H_2$ (with flow rates of 200/20/40 standard cubic centimeter per minute (sccm), respectively) was introduced as the feeding gas. After 30–50 min of growth (figure 1(h)), the gas supply was stopped, and the system gradually cooled down to room temperature, then the sample was taken out for various characterizations.

3. Results and discussion

Typical SEM images of as-grown HADCNTs are shown in figure 2, they are all horizontally well aligned with one end anchored to the trench sidewall, and the other either suspended in air or in contact with another sidewall, thus these CNT bundles could be regarded as CNT cantilevers/bridges. Figures 2(a) and (b) demonstrate two almost parallel HADCNT thin films spanning a 20 μm wide trench from the right trench sidewall in different perspectives, with part of their free ends in contact with the opposite trench sidewall. Note that the lower film is just about 300 nm thick but is still suspended horizontally for over 15 μm before the occurrence of evident downward deflection. Figure 2(c) shows a HADCNT bundle grown from almost the whole left sidewall, and these CNTs are not equal in length due to the uneven distribution of Fe catalyst film thickness generated in the tilt angle deposition process. Figure 2(d) is a localized view of these CNTs. A slender HADCNT bundle and its central magnified view are revealed in figures 2(e) and (f) respectively. The sharp turning of the right end comes from the sudden termination of the gas supply at the end of the growth process, which causes a dramatic pressure change inside the chamber, together with the adhesion between the CNTs and the trench sidewall; the 'free' end of the bundle finally gets in contact with the sidewall, giving rise to a CNT bridge. From local magnified views in figures 2(d) and (f), the linear packing density of these CNTs is shown to be about 10 CNTs μm^{-1}, which is much denser than those orientated by crystal lattice/atomic steps [13–17] or external fields [18, 19]. It should be noted that catalyst patterns on sidewalls are not defined by photolithography; instead, they were generated during the ultrasonic cleaning of photoresist, when part of the catalyst film was simultaneously removed from the trench sidewall.

The very good horizontal alignment of these CNTs could be attributed mainly to van der Waals interaction among CNTs in the bundle. It has been found that the van der Waals attraction could be neglected as long as the intertube distance is larger than the CNT diameter [22], thus strong attraction mainly appears at CNT contacts. As shown in figures 2(d) and (f), CNTs obtained here are wavy due to the gas flow fluctuations, and they get entangled and contacted with neighbors frequently along their length directions. The van der Waals attraction between two contacted CNTs is about 0.36 nN per unit length [23], which is over 100 times larger than a

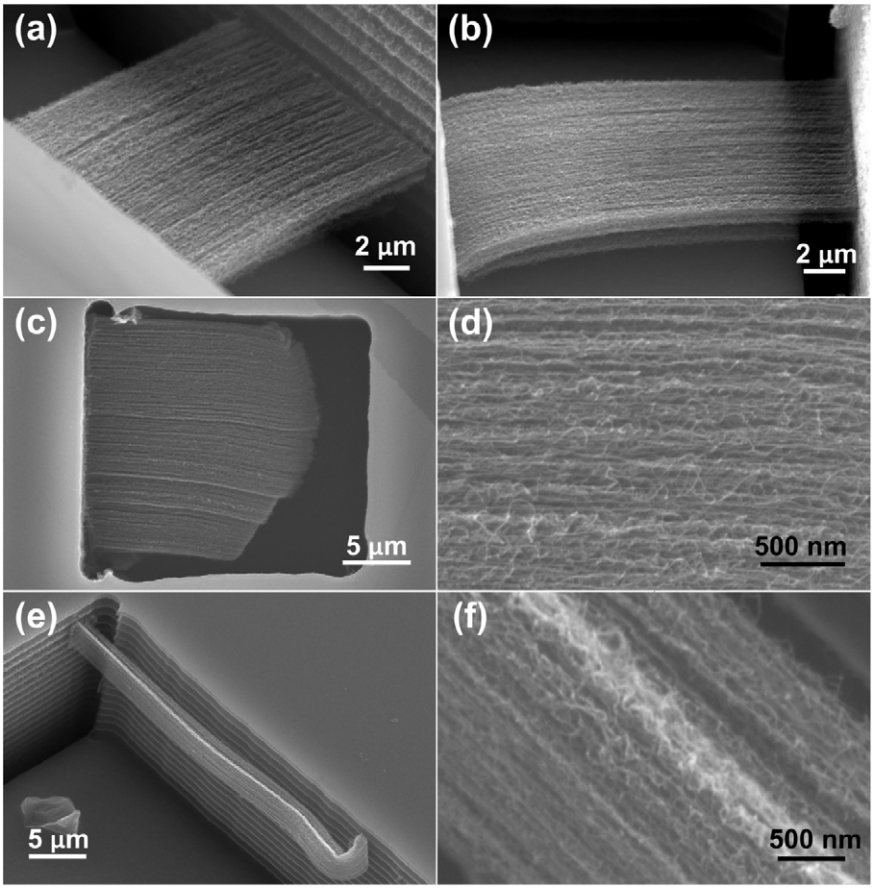

Figure 2. Typical as-grown HADCNTs: (a) a thin film HADCNTs across the trench and (b) its tilt side view; (c) a fat CNT cantilever grown from almost the whole left sidewall of the trench, and (d) its magnified view; (e) the slender CNT cantilever with an aspect ratio of about 25; (f) the local view of its central part. The trench ripples come from the etching–passivation cycles of the DRIE process.

CNT's gravity, thus a CNT could be held by its neighbors against its gravity. On the other hand, for a single trench unit, the catalyst layer was deposited within the same batch, and CNTs were grown under the same conditions, thus the growth rate of these CNTs is almost the same. Therefore, on the whole, these dense CNTs grow side by side like a large single material block, and they extrude horizontally (or perpendicular to their vertical catalyst plane) during their growth. The well studied vertically aligned dense CNTs bundles [24, 25] and forests [26] align vertically in a similar way. For an isolated single CNT or sparse CNTs (where the van der Waals effect could be neglected), they will eventually collapse to the trench bottom when it grows some micrometers long due to its gravity, which can be seen in figure 3, agreeing well with the prediction by Marcus *et al* [27]. Therefore, sparse CNTs grown with solution precursor usually lie on the substrate after growth [10–12].

To conduct electrical characterization on a typical HADCNT bundle in figure 2(e), the FEI Nova NanoLab 200 DualBeam SEM/focused ion beam (FIB) system was applied to deposit a 8 μm(length) $\times$ 5 μm(width) $\times$ 0.2 μm (thickness) tungsten layer near each bundle end as the electrodes, and a 3.5 μm (length) $\times$ 3 μm (width) $\times$ 0.5 μm (thickness) tungsten (W) layer to cover the steps between the CNT bridge ends and electrodes. After that, about 13 s of XeF_2 cleaning was conducted to remove the possible overflow of W particles

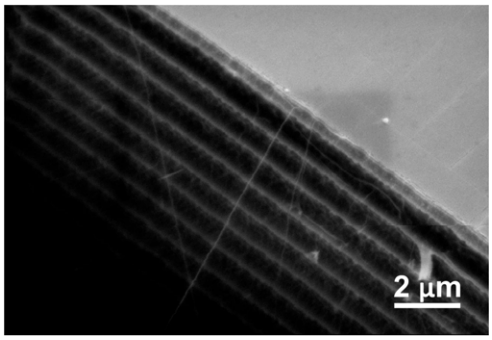

Figure 3. Isolated CNTs grown from the trench sidewall.

in case of short circuit during measurement (figure 4(a)). Then, the electrodes were connected to a pair of W probes (with a tip diameter of about 1 μm) on a probe station. The resultant current–voltage (I–V) characteristic curve is shown in figure 4(b), which indicates that the HADCNT bundle is in good (but not ohmic) contact with W electrodes and is of metallic nature. Taking the effective contact area into account, the estimated resistivity of the CNT bridge is about 0.0072 Ω cm, which is about 25% smaller than our previous through-silicon CNT bundles [24] and vertical CNT

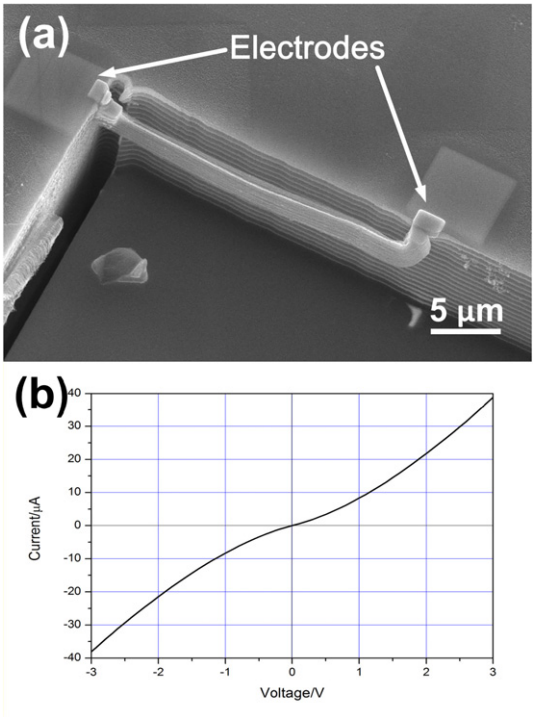

Figure 4. (a) The HADCNT bundle before the I–V measurement and (b) the corresponding I–V curve.

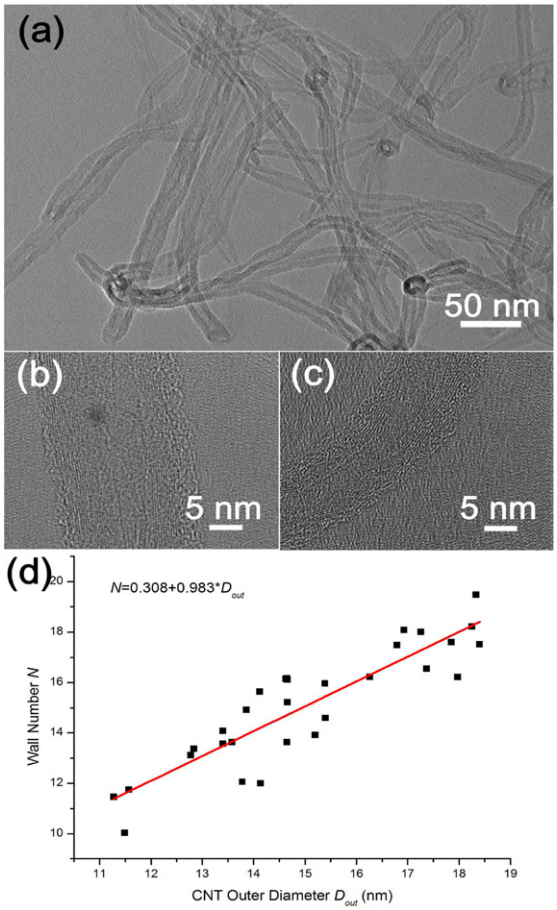

Figure 5. (a) TEM image of HADCNTs; (b) and (c) are HRTEM images of two CNTs with different outer diameters; (d) the relationship between MWCNT diameter and wall numbers.

bundles [28], though the total resistance of the slender CNT bridge here is about 30 times larger. This mainly results from its much smaller cross-sectional area (just $\sim$5 μm^2) and better contact to external probes by electrodes. However, the resistivity here is still several orders of magnitude larger than that of bulk copper. Firstly, the FIB deposited electrodes only cover the upper CNTs in the bundle, while the electron hopping between individual CNTs is much more difficult than the electron longitudinal transport within CNTs, thus only a fraction of CNTs contribute to the electrical conduction; on the other hand, the electrodes touch CNTs' sides instead of their ends (now in contact with the trench sidewall), which also gives rise to a large contact resistance. Therefore, it is encouraging to grow CNTs directly between electrodes deposited on trench sidewalls, and explore the solutions to increase the packing density of CNT bundles.

The HRTEM image (model: JEOL JEM-2010) in figure 5(a) reveals that these CNTs are all multiwalled CNTs (MWCNTs) with an outer diameter D_{out} of 10–20 nm. The average outer diameter of these CNTs is about 15 nm, and the inner/outer diameter ratio is within the range of 0.24–0.4. Large MWCNTs are found to contain more CNT walls, and this is also indicated in figures 5(b) and (c), which compare two MWCNTs of different outer diameters (19.7 nm and 11.5 nm respectively) and wall numbers (19 and 9 respectively). Figure 5(d) depicts the relationship between CNT wall number N and outer diameter D_{out}, which could roughly be approximated by $N = 0.308 + 0.983 \times D_{\text{out}}$. CNT outer diameter is usually decided by its catalyst particle dimension [29], and a larger catalyst usually lead to CNTs with larger diameters, while a larger catalyst has a larger catalytically effective exposed area [30, 31] during the growth, therefore, large MWCNTs usually contain more CNT walls. More CNT walls means more conduction channels for electrons and heat along the CNTs, thus better electrical and thermal conductivity of MWCNTs could be expected [32]. The phenomenon indicates a possible solution to tune the electrical and thermal properties of MWCNTs by controlling their diameters during their growth.

The growth of HADCNTs allows the measurement of the CNTs' quality difference along CNTs using Raman spectroscopy, which was conducted at the HADCNT roots, middle parts, and tips by a Renishaw Raman Microprobe-RM1000 with a laser wavelength of 633 nm. It has been widely accepted that the D band at $\sim$1350 cm^{-1} originates from defects in CNTs, and the G band at $\sim$1580 cm^{-1} represents the crystalline hybridized sp^2 graphene structure, thus the peak intensity ratio of $I_{\text{G}}/I_{\text{D}}$ could provide a good measure of CNT structure quality or its graphitization degree [33]. As shown in figure 6, from HADCNTs' roots to tips, the D band becomes relatively weaker and weaker, and the intensity ratio $I_{\text{G}}/I_{\text{D}}$ gradually increases from 0.99 at the CNT root to 1.16 at the tip, indicating a longitudinally improved CNT crystallinity. This trend was confirmed by Raman spectroscopy on many other HADCNT bundles. We traced this phenomenon back

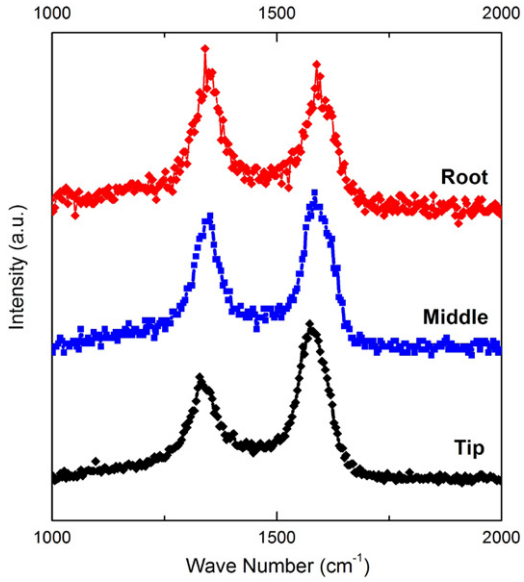

Figure 6. A typical Raman spectrum taken from the root, middle, and tip of the HADCNTs.

to the CNT growth process. In the beginning, C_2H_2 gas is absorbed by a Fe catalyst particle, the accumulating absorption leads to the supersaturation of carbon atoms and then the precipitation of CNTs. However, the carbon supply rate seems to be much larger than CNT precipitation rate, thus high defect concentration will be present around the catalyst [34]; as CNTs extrude, parts of the defects (especially those around the CNT tips) will be repaired during the annealing process, which has been confirmed by both quantum mechanics simulation [35] and *in situ* Raman spectroscopy [36]. The process gives rise to a defect concentration gap between the CNT root and tip, thus leading to the propagation of defects [34, 37] toward CNT tips at high growth temperature. Therefore, there is a defect gradient along CNTs, and accordingly, the Raman intensity ratio I_G/I_D gradually decreases from their roots to tips. This may open a new perspective regarding the quality control of CNTs during their growth.

4. Conclusion

In conclusion, we have demonstrated a feasible solution to grow HADCNTs in the form of CNT cantilevers/bridges from designated trench sidewalls with a conventional CVD growth method. The Fe catalysts were deposited onto the selected trench sidewall by tilt angle electron beam evaporation. The CNT linear packing density in resultant HADCNTs is about 10 CNTs μm^{-1}. The good horizontal alignment is mainly attributed to the van der Waals effect within the dense CNT bundle. The as-grown CNTs are MWCNTs with outer diameters of 10–20 nm, and generally, large MWCNTs contain more CNT walls, therefore it is possible to tune the electrical and thermal conductivity of CNTs. The Raman spectra along HADCNTs present an increasing intensity ratio I_G/I_D from CNT roots to their tips, indicating the existence of a defect gradient along CNTs. Further efforts are to be conducted to improve the CNT quality and their electrical performance. Compared with most other methods to grow HADCNTs, the solution here is more practical, because it does not involve the introduction of external electric/magnetic field, and the as-grown CNTs are horizontally suspended, free of interaction with the substrate, thus making these CNT cantilevers/bridges promising in micro/nanoelectronics (including transistors and interconnects) and biochemical sensor applications.

Acknowledgments

We would like to thank all the staff and students in Micromachines Lab 1 for the fabrication and characterizations of HADCNTs, and we gratefully acknowledge Mr Tian Fook Kong and Professor Wen Siang Lew in the School of Physical and Mathematical Sciences for Fe catalyst deposition, Dr Chuanwei Chen and Professor Hongjin Fan in the School of Physical and Mathematical Sciences for Al_2O_3 layer deposition, and Dr Zipeng Li in the School of Material Science and Engineering for the TEM characterization.

References

[1] Zhang T, Mubeen S, Myung N V and Deshusses M A 2008 *Nanotechnology* **19** 332001
[2] Brahim S, Colbern S, Gump R, Moser A and Grigorian L 2009 *Nanotechnology* **20** 235502
[3] Wang Y, Zhou Z, Yang Z, Chen X, Xu D and Zhang Y 2009 *Nanotechnology* **20** 345502
[4] Baughman R H *et al* 1999 *Science* **284** 1340–4
[5] Aliev A, Oh J, Kozlov M, Kuznetsov A, Fang S, Fonseca A, Ovalle R, Lima M, Haque M and Gartstein Y 2009 *Science* **323** 1575
[6] Sul O and Yang E H 2009 *Nanotechnology* **20** 095502
[7] Pugno N 2006 *J. Phys.: Condens. Matter* **18** S1971
[8] Moriyama N, Ohno Y, Kitamura T, Kishimoto S and Mizutani T 2010 *Nanotechnology* **21** 165201
[9] Yan F, Zhang C, Cott D, Zhong G and Robertson J 2010 *Phys. Status Solidi* b **247** 2669–72
[10] Wen Q, Qian W, Nie J, Cao A, Ning G, Wang Y, Hu L, Zhang Q, Huang J and Wei F 2010 *Adv. Mater.* **22** 1867–71
[11] Li W, Xie S, Qian L, Chang B, Zou B, Zhou W, Zhao R and Wang G 1996 *Science* **274** 1701
[12] Campos-Delgado J, Maciel I, Cullen D, Smith D, Jorio A, Pimenta M, Terrones H and Terrones M 2010 *ACS Nano* **4** 1696–702
[13] Su M, Yan Li, Maynor B, Buldum A, Lu J P and Liu J 2000 *J. Phys. Chem.* B **104** 6505–8
[14] Yuan D, Ding L, Chu H, Feng Y, McNicholas T P and Liu J 2008 *Nano Lett.* **8** 2576–9
[15] Ago H, Nishi T, Imamoto K, Ishigami N, Tsuji M, Ikuta T and Takahashi K 2010 *J. Phys. Chem.* C **114** 12925–30
[16] Maret M, Saubat B, Flock J, Mantoux A, Charlot F and Makarov D 2010 *Chem. Phys. Lett.* **495** 96–101
[17] Xiao J *et al* 2009 *Nano Lett.* **9** 4311–9
[18] Lee K-H, Cho J-M and Sigmund W 2003 *Appl. Phys. Lett.* **82** 448
[19] Chai Y, Xiao Z and Chan P 2010 *Nanotechnology* **21** 235705
[20] Cao A, Baskaran R, Frederick M J, Turner K, Ajayan P M and Ramanath G 2003 *Adv. Mater.* **15** 1105–9
[21] Talapatra S, Kar S, Pal S K, Vajtai R, Ci L, Victor P, Shaijumon M M, Kaur S, Nalamasu O and Ajayan P M 2006 *Nat. Nanotechnol.* **1** 112–6
[22] Girifalco L A, Hodak M and Lee R S 2000 *Phys. Rev.* B **62** 13104

[23] Chen B, Gao M, Zuo J, Qu S, Liu B and Huang Y 2003 *Appl. Phys. Lett.* **83** 3570
[24] Xu T, Wang Z, Miao J, Chen X and Tan C 2007 *Appl. Phys. Lett.* **91** 042108
[25] Xu T, Miao J, Li H and Wang Z 2009 *Nanotechnology* **20** 295303
[26] Lee D H, Lee W J and Kim S O 2009 *Nano Lett.* **9** 1427–32
[27] Marcus M S, Simmons J M, Baker S E, Hamers R J and Eriksson M A 2009 *Nano Lett.* **9** 1806–11
[28] Jun-Tae K, Hyun-Woo R and Jung-Hyun P 2008 *Japan. J. Appl. Phys.* **47** 4803–6
[29] Cheung C L, Kurtz A, Park H and Lieber C M 2002 *J. Phys. Chem.* B **106** 2429–33
[30] Lee D H, Kim S O and Lee W J 2010 *J. Phys. Chem.* C **114** 3454–8
[31] Choi K M, Augustine S, Choi J H, Lee J H, Shin W H, Yang S H, Lee J Y and Kang J K 2008 *Angew. Chem. Inter. Edn* **47** 9904–7
[32] Naeemi A and Meindl J D 2009 *Annu. Rev. Mater. Res.* **39** 255–75
[33] Dresselhaus M S, Dresselhaus G, Saito R and Jorio A 2005 *Phys. Rep.* **409** 47–99
[34] Hofmann S, Sharma R, Ducati C and Du G 2007 *Nano Lett.* **7** 602–8
[35] Deng W Q, Xu X and Goddard W A III 2004 *Nano Lett.* **4** 2331–5
[36] Kaminska K, Lefebvre J, Austing D G and Finnie P 2007 *Nanotechnology* **18** 165707–12
[37] Ding F, Jiao K, Lin Y and Yakobson B I 2007 *Nano Lett.* **7** 681–4